

INTERSTELLAR ENVIRONMENTS PROBED BY Ca I ABSORPTION AND THE EFFECTS  
OF DENSITY-DEPENDENT DEPLETIONSJASON A. CARDELLI,<sup>1</sup> S. R. FEDERMAN,<sup>2</sup> AND V. V. SMITH<sup>3</sup>*Received 1991 July 23; accepted 1991 August 14*

## ABSTRACT

The environments where absorption from interstellar Ca I arises have been studied. For lines of sight containing clouds of moderate density, such as those toward Cep OB3, the line profiles of Ca I and CH<sup>+</sup> are very similar. However, they differ significantly from that for CH, which probes denser molecular gas. When normalized to the column density of CH, the column densities of CN, a molecule that samples relatively dense gas, and Ca I are inversely related. Thus, regions showing strong absorption of Ca I (and CH<sup>+</sup>) are different from those with strong CH and CN absorption. In the case for Ca I, the dependence of calcium depletion on density is the cause for the observed trends. In dense gas the depletion is so severe that absorption from neutral calcium may be below detection limits. These results are expected to apply equally well to other elements, particularly those displaying large gas-phase depletions.

*Subject headings:* interstellar: abundances — interstellar: grains — interstellar: matter

## 1. INTRODUCTION

Interstellar absorption lines from neutral atomic species, whose ionization potentials are less than 13.6 eV, are usually interpreted as arising from relatively dense material. This belief is based on the premise that ionization balance controls the concentration of neutral species. Under conditions appropriate to ionization equilibrium, the density of neutral atomic gas,  $n(X\ I)$ , is proportional to the square of the density of hydrogen nuclei. One factor of gas density comes from the density of the dominant ionization stage, which is most often singly ionized atoms; the other factor comes from the density of electrons. Although this picture is probably appropriate for lines of sight passing through low-density, neutral gas, in this *Letter* we show that the density dependence of gas-phase depletion onto grains must be considered when describing the situation in denser, molecular gas.

Our revised picture arose from analysis of absorption from gas in the direction of stars in the Cepheus OB3 association. Section 2 describes the observations made toward HD 217086 and HD 217312. We discuss our interpretation of the spectra for these directions and provide additional evidence for our hypothesis in § 3. The last section summarizes our findings.

## 2. DATA

High-resolution spectra were obtained at McDonald Observatory with the coude spectrometer of the 2.7 m telescope. Either a Texas Instruments 800 × 800 chip with 15 × 15 μm pixels, or a Tektronix 512 × 512 chip with 27 × 27 μm pixels, was used as the detector. The camera setup yielded an approximate dispersion of 0.6 Å mm<sup>-1</sup>. Two wavelength regions were observed, one at 4230 Å for CH<sup>+</sup> λ4232.54 and Ca I λ4226.73, and one at 4300 Å for CH λ4300.3. For the Tektronix chip, the exact dispersion was 0.017 Å pixel<sup>-1</sup> at both 4230 and 4300 Å, while the TI chip gave a dispersion of 0.0094 Å pixel<sup>-1</sup>. The resolution for the spectra was determined by the spectrometer

entrance slit, which was set to 3 pixels for the Tektronix chip (or 0.051 Å resolution) and 6 pixels for the TI chip or 0.057 Å resolution).

The spectra were reduced to final form using the NOAO reduction package IRAF. Bias frames taken on the same night as the program spectra were subtracted from the image frames, and the resultant program frames were flattened with a continuum lamp source. The bias-subtracted, flattened frames were then reduced to one-dimensional spectra using the optimal extraction routine in IRAF. Finally the spectra were reduced to a laboratory wavelength scale using a Th-Ar hollow cathode as a wavelength standard. Final residuals in the fit to wavelength were typically 0.01 Å, or 0.7 km s<sup>-1</sup>.

Some examples of the observed line profiles for two stars in the Cep OB3 complex, HD 217312 [ $E(B-V) = 0.66$  mag] and HD 217086 [ $E(B-V) = 0.96$  mag], are shown in Figures 1 and 2. The data have been normalized to a continuum of unity; the velocity scales are heliocentric. All the data for HD 217312 were obtained with the TI chip and were binned to two samples per resolution element to improve the signal to noise with no loss in resolution.

## 3. RESULTS AND DISCUSSION

The interstellar spectra shown in Figures 1 and 2 reveal that the Ca I and CH<sup>+</sup> profiles are remarkably similar, but yet distinct from the CH profile. The CH radical is known to sample gas consisting in large measure of molecular hydrogen. Optical and radio observations of CH (Federman 1982; Mattila 1986) in gas with visual extinctions approaching 4 mag indicate that the column density of CH,  $N(\text{CH})$ , is linearly proportional to  $N(\text{H}_2)$ . The association of simple heavy-element-bearing molecules with gas containing molecular hydrogen is expected because reactions involving molecular hydrogen lead to the production of these molecules (e.g., van Dishoeck & Black 1986). The presence of relatively dense gas when the amounts of H<sub>2</sub> are substantial is a consequence of the process whereby H<sub>2</sub> shields itself from photodissociation (see Federman, Glassgold, & Kwan 1979). The association of absorption from CH<sup>+</sup> and dense gas, however, is not strong.

The observed values for  $N(\text{CH}^+)$  cannot be reproduced by

<sup>1</sup> Department of Astronomy, University of Wisconsin, Madison, WI 53706.<sup>2</sup> Department of Physics and Astronomy, University of Toledo, Toledo, OH 43606.<sup>3</sup> Department of Astronomy, University of Texas, Austin, TX 78712.

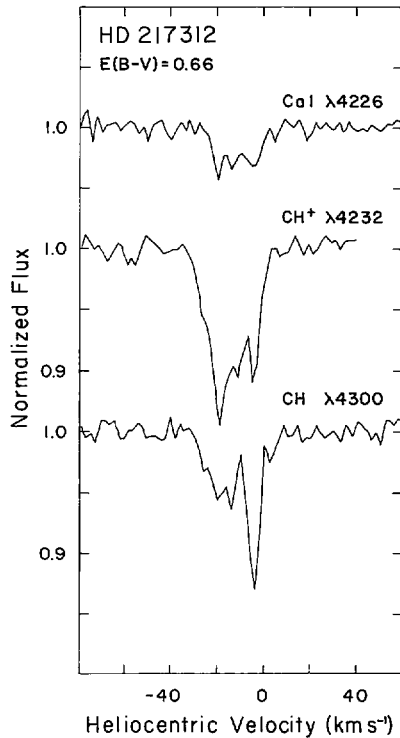


FIG. 1.—Absorption from interstellar Ca I, CH<sup>+</sup>, and CH in the spectrum of HD 217312, which is normalized to unity for the stellar continuum.

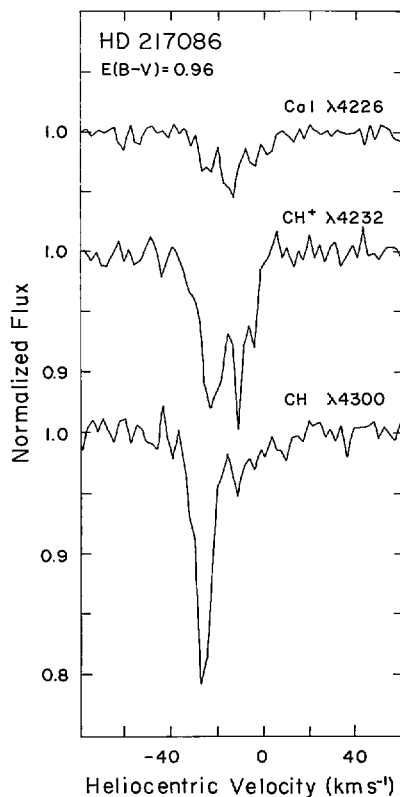


FIG. 2.—Same as Fig. 1 for HD 217086

the chemical schemes that are successful in reproducing many of the observations for neutral molecules (van Dishoeck & Black 1986). Although inconsistencies still persist, the most promising chemical models incorporate CH<sup>+</sup> production behind a shock wave (Elitzur & Watson 1980; Draine & Katz 1986; Pineau des Fôrets et al. 1986). In these models, CH<sup>+</sup> production occurs in relatively low-density, kinematically hot gas just behind the shock, not farther downstream where compression leads to significant increases in density. This fact arises because in regions of high density (1) the destructive chemical attack of CH<sup>+</sup> is enhanced and (2) the formation of the molecule is suppressed when cooling times are short. Because of the similarity between the profiles of Ca I and CH<sup>+</sup> absorption in Figures 1 and 2, the substantial amounts of Ca I at low densities suggests that something in addition to simple ionization balance is taking place.

The ideas are illustrated in a more comprehensive way in Figure 3, where  $\log [N(\text{CN})/N(\text{CH})]$  is plotted against  $\log [N(\text{Ca I})/N(\text{CH})]$ . The data come from several sources. For the directions specified in the figure, the sources of the data are Crutcher (1985) for HD 29647, Cardelli et al. (1990) for HD 62542, and Federman, Danks, & Lambert (1984) and Lambert & Danks (1986) for  $\mu$  Nor. The remaining data come from the work of Chaffee & Dunham (1979), Frisch (1979), Federman & Hobbs (1983), Federman et al. (1984), Cardelli & Wallerstein (1986), Lambert & Danks (1986), Cardelli & Wallerstein (1989), and Hawkins & Meyer (1989).

Because CN is formed after significant amounts of CH have been produced (Federman et al. 1984), CN traces relatively dense material (see Joseph et al. 1986). The column densities of Ca I and CN are normalized to  $N(\text{CH})$  because CH samples regions of molecular hydrogen. Moreover, the rate equations for Ca I, CH, and CN (see eqs. [4], [6], and [7]) each contain a photochemical term, and the normalization process then allows us to factor out uncertainties associated with this term. Figure 3 shows that CN and Ca I are *inversely* related, not directly proportional as would be expected from ionization balance for calcium and chemical models of CN. Such a varia-

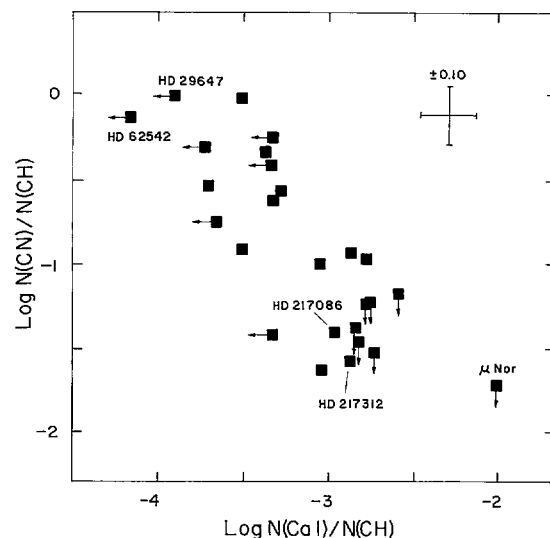


FIG. 3.—Plot of  $\log [N(\text{CN})/N(\text{CH})]$  vs.  $\log [N(\text{Ca I})/N(\text{CH})]$ . Extreme cases and the two stars studied here are indicated. Moderately low-density gas, from which little or no CN absorption is detected, occupies the lower portion of the figure. The error bars represent  $\sigma$  in  $\log N$  of 0.1 dex.

tion between CN and Ca I resembles Figure 6 of Cardelli et al. (1990) where CN is compared with CH<sup>+</sup>. Thus, Ca I and CH<sup>+</sup> appear to be tracing material that is distinct from gas containing CN. We discussed the reason for the lack of a correspondence between CN and CH<sup>+</sup> above; we now show that the lack of a correspondence with Ca I arises because depletion must be taken into account.

In light of the results from Figure 3, an analysis of the rate equations for Ca I, CN, and CH reveals that the calcium concentration varies inversely with gas density. The equation for Ca I is based on ionization balance

$$n(\text{Ca I}) = \frac{\alpha n(\text{Ca II})n(e)}{\Gamma(\text{Ca I})}, \quad (1)$$

where  $n(X)$  is the space density of species  $X$ ,  $\alpha$  is the electron recombination rate constant for Ca II, and  $\Gamma(\text{Ca I})$  is the ionization rate for neutral calcium. Equation (1) can be rewritten upon substitution of the following expressions for  $n(\text{Ca II})$  and  $n(e)$ ,

$$n(\text{Ca II}) = A(\text{Ca})10^{\delta(\text{Ca})}n, \quad (2)$$

$$n(e) \sim n(\text{C}^+) = A(\text{C})10^{\delta(\text{C})}fn. \quad (3)$$

Here  $A(X)$  and  $\delta(X)$  are the cosmic abundance and logarithmic depletion for element  $X$ ,  $f$  is the fractional ionization for carbon, which is the dominant source for electrons in diffuse clouds, and  $n$  is the density of hydrogen nuclei. The equation for Ca I takes the form

$$n(\text{Ca I}) = \frac{K_1 n^{[2 - d(\text{Ca}) - d(\text{C})]}}{\Gamma(\text{Ca I})} \quad (4)$$

with  $K_1$  a constant when we incorporate the dependence of depletion on density as

$$10^{\delta(X)} \propto n^{-d(X)} \quad (5)$$

(e.g., see Jenkins 1987). Chemical analysis (Federman et al. 1984; Federman & Huntress 1989) leads to rate equations for CH and CN that have the simplified forms with reference to equation (3)

$$n(\text{CH}) = \frac{K_2 n^{[1 - d(\text{C})]}}{\Gamma(\text{CH})}, \quad (6)$$

$$n(\text{CN}) = \frac{K_3 n^{[3 - d(\text{C})]}}{\Gamma(\text{CN})}. \quad (7)$$

For the molecules, the chemistries are initiated by reactions involving C<sup>+</sup>, and the  $\Gamma$ 's are photodissociation rates.

As described previously, normalizing the space densities for Ca I and CN to that for CH allows us to focus our attention on gas containing H<sub>2</sub>, and it minimizes the variations associated with the photorates. The combination of equations (4), (6), and (7) leads to

$$\frac{n(\text{Ca I})}{n(\text{CH})} \propto n^{[1 - d(\text{Ca})]}, \quad (8)$$

$$\frac{n(\text{CN})}{n(\text{CH})} \propto n^2. \quad (9)$$

With the assumption that space densities and column densities have the same functional form, we arrive at our final expression:

$$\log \frac{N(\text{CN})}{N(\text{CH})} \propto \frac{2}{[1 - d(\text{Ca})]} \log \frac{N(\text{Ca I})}{N(\text{CH})}. \quad (10)$$

Our assumption is probably valid because the outer regions of molecular clouds have space densities increasing monotonically with depth into a cloud (de Jong, Dalgarno, & Boland 1980; Boland & de Jong 1984). A fit to the data in Figure 3 reveals a slope of  $\sim -1.0$ . The upper limits are treated the same because it is our belief that they represent actual values to within a factor of a few, or  $\leq 0.5$  dex. From our analysis and the slope derived from Figure 3, we infer a value for  $d(\text{Ca})$  perhaps as large as  $\sim 3.0$ .

A value for  $d(\text{Ca})$  as large as 3.0 indicates that the dependence of depletion on density is quite steep in the densest gas encountered by optical means. From his analysis of the interstellar spectrum toward HD 29647 ( $A_V \sim 4$  mag), which samples the dense envelope of the Taurus molecular cloud 1, Crutcher (1985) found that sulfur is depleted by at least a factor of 10. This contrasts with the results for typical, low-density diffuse clouds where sulfur appears to be only slightly depleted. Moreover, he noted that the Ca II H and K lines seen in the spectrum are probably stellar. Meyers et al. (1985) also observed enhanced depletion in moderately dense gas associated with the passage of a shock through the cloud in front of the bright stars in the Sco OB2 association. The sight lines studied by them are represented in Figure 3 by data with upper limits to  $N(\text{CN})/N(\text{CH})$ , or in other words, the directions with the *lowest* density gas in our sample. They found that iron was depleted by an additional factor of 2 in the denser, post-shock gas relative to the preshock gas. This is an appreciable enhancement for gas of only moderate density. Thus, significant amounts of depletion appear to take place in dense regions.

For measurements sampling a line of sight, the abundances of calcium and titanium are expected to behave in a similar way with density. Jenkins (1987) found that  $d(\text{Ti})$  is  $\sim 0.85$  when average line-of-sight densities are considered, while we find that  $d(\text{Ca})$  is  $\sim 3$ . Although our value is significantly larger than that of Jenkins, the results are not necessarily inconsistent. The likely cause for the difference centers on the fact that the data shown in Figure 3 are probably a more direct probe of density variations than the data used by Jenkins. Our sample stresses the regions where only molecules and/or neutral atoms exist, while the data of Jenkins includes the entire sightline. An additional effect may also be playing a role: Jenkins (1987) relied on data for Ti II, which may predominantly sample warm intercloud gas (Joseph & Jenkins 1991).

#### 4. CONCLUSIONS

The amount of Ca I absorption depends on the amount of calcium depletion, which in turn is a sensitive function of density. The line profiles for Ca I from spectra of stars in Cep OB3 do not resemble those for CH, which samples relatively dense, molecular gas, but instead are very similar to the profiles of the CH<sup>+</sup> line. Since dense gas restricts the abundance of CH<sup>+</sup>, the correspondence between Ca I and CH<sup>+</sup> suggests that absorption from these two species arises from gas with relatively low density. The inverse relationship between

$\log [N(\text{CN})/N(\text{CH})]$  and  $\log [N(\text{Ca I})/N(\text{CH})]$  is also consistent with this picture. The empirically derived slope of  $\sim -1.0$  suggests that calcium depletion varies roughly as  $n^{-3}$  in moderately dense, molecular gas. A shallower dependence on density may apply to low-density gas probed by absorption from the dominant ion (Jenkins 1987). A preliminary analysis for K I indicates that our results for calcium may pertain to other atomic species also.

J. A. C. was supported by NASA contract NAS 5-29638, and S. R. F. was supported under the NASA RTOPs program and funded through the Jet Propulsion Laboratory; and V. V. S. was supported by grants from the Robert A. Welch Foundation of Houston, Texas, and from the National Science Foundation (AST89-02835).

## REFERENCES

- Boland, W., & de Jong, T. 1984, *A&A*, 134, 87  
 Cardelli, J. A., Sunteff, N. B., Edgar, R. J., & Savage, B. D. 1990, *ApJ*, 362, 551  
 Cardelli, J. A., & Wallerstein, G. 1986, *ApJ*, 302, 492  
 ———. 1989, *AJ*, 97, 1099  
 Chaffee, F. H., & Dunham, T. 1979, *ApJ*, 233, 568  
 Crutcher, R. M. 1985, *ApJ*, 288, 604  
 de Jong, T., Dalgarno, A., & Boland, W. 1980, *A&A*, 91, 68  
 Draine, B. T., & Katz, N. 1986, *ApJ*, 306, 655  
 Elitzur, M., & Watson, W. D. 1980, *ApJ*, 236, 172  
 Federman, S. R. 1982, *ApJ*, 257, 125  
 Federman, S. R., Danks, A. C., & Lambert, D. L. 1984, *ApJ*, 287, 219  
 Federman, S. R., Glassgold, A. E., & Kwan, J. 1979, *ApJ*, 227, 466  
 Federman, S. R., & Hobbs, L. M. 1983, *ApJ*, 265, 813  
 Federman, S. R., & Huntress, W. T. 1989, *ApJ*, 338, 140  
 Frisch, P. 1979, *ApJ*, 227, 474  
 Hawkins, I., & Meyer, D. M. 1989, *ApJ*, 338, 888  
 Jenkins, E. B. 1987, in *Interstellar Processes*, ed. D. J. Hollenbach & H. A. Thronson (Dordrecht: Reidel), 533  
 Joseph, C. L., & Jenkins, E. B. 1991, *ApJ*, 368, 201  
 Joseph, C. L., Snow, T. P., Seab, C. G., & Crutcher, R. M. 1986, *ApJ*, 309, 771  
 Lambert, D. L., & Danks, A. C. 1986, *ApJ*, 303, 401  
 Mattila, K. 1986, *A&A*, 160, 157  
 Meyers, K. A., Snow, T. P., Federman, S. R., & Breger, M. 1985, *ApJ*, 288, 148  
 Pineau des Forêts, G., Flower, D. R., Hartquist, T. W., & Dalgarno, A. 1986, *MNRAS*, 220, 801  
 van Dishoeck, E. F., & Black, J. H. 1986, *ApJS*, 62, 109